

# Computer Modeling of Drug Distribution after Intravitreal Administration

N. Haghjou, M. J. Abdekhodaie, Y. L. Cheng, M. Saadatmand

**Abstract**—Intravitreal injection (IVI) is the most common treatment for eye posterior segment diseases such as endophthalmitis, retinitis, age-related macular degeneration, diabetic retinopathy, uveitis, and retinal detachment. Most of the drugs used to treat vitreoretinal diseases, have a narrow concentration range in which they are effective, and may be toxic at higher concentrations. Therefore, it is critical to know the drug distribution within the eye following intravitreal injection. Having knowledge of drug distribution, ophthalmologists can decide on drug injection frequency while minimizing damage to tissues. The goal of this study was to develop a computer model to predict intraocular concentrations and pharmacokinetics of intravitreally injected drugs. A finite volume model was created to predict distribution of two drugs with different physiochemical properties in the rabbit eye. The model parameters were obtained from literature review. To validate this numeric model, the in vivo data of spatial concentration profile from the lens to the retina were compared with the numeric data. The difference was less than 5% between the numerical and experimental data. This validation provides strong support for the numerical methodology and associated assumptions of the current study.

**Keywords**—Posterior segment, Intravitreal injection (IVI), Pharmacokinetic, Modelling, Finite volume method.

## I. INTRODUCTION

THE aging of the general population, along with the higher incidences of eye diseases, such as age-related macular degeneration (AMD) or retinal edema, has created a need to deliver drugs to the posterior segment i.e. vitreous, retina and choroid (Fig. 1) [1]. Due to the physiological barriers within the eye, drug delivery to the posterior segment is a challenge and most drugs fail to reach therapeutic levels in this region after topical and systemic administration [2]. Currently, direct intravitreal injection (IVI) is the most common approach used to deliver posterior levels of drugs in humans. Drugs introduced by this route include anti-infectives, tissue plasminogen activator, pegaptanib, ranibizumab, P2Y2 receptor agonist, adenoviral vector for pigment epithelium derived factor and triamcinolone [3].

The duration of effects of an intravitreally administered drug depends on the retention of the injected drug at the site of

administration. The higher the intravitreal half-life of a drug injected in the vitreous of the eye, the greater is the anticipated duration of the pharmacological response. Longer half-life of a drug makes it amenable for less frequent dosing [4]. It is time consuming and cost intensive to determine the intravitreal half-life of each drug in vivo. So, a mathematical model is essential for the development of therapeutic agents with desired half-lives and other intravitreal pharmacokinetic properties. On the other hand, many drugs, which are used to treat vitreoretinal diseases, have a narrow concentration range in which they are effective, and may be toxic at higher concentrations [5]. Therefore, it is critical to know the drug distribution within the eye following intravitreal injection. The ability to predict drug distribution can maximize the therapeutic benefits while minimizing damage to tissues caused by excessively high concentrations of drugs.

Using realistic geometries and ocular properties, a finite volume model has been developed to study drug distribution and elimination pathway after an intravitreal injection.

## II. GEOMETRICAL MODEL

The geometrical model adapted in this study, shown in Fig. 2, is based on the physiological dimensions of rabbit eye in accordance with the model presented by Friedrich et al. [6]. The rabbit eye was initially chosen rather than the human eye due to the availability of experimental data for confirmation of model calculations. There are three main tissues that bound the vitreous humor: the retina, lens and hyaloid membrane. The radius of curvature of the vitreous (and inner retina) is 7.8mm. The hyaloid membrane is 3.1 mm behind the center of curvature of the vitreous. The lens is modeled as a section of sphere with 6 mm radius. The distance between lens and retina center is 6.2 mm.

## III. GRID GENERATION

Because the vitreous is symmetrical about an axis that passes through the center of the lens and the vitreous, the 2D axis-symmetric geometry of the rabbit eye is generated using the commercial software Gambit 2.2.30. The vitreous chamber can be generated by rotating the model 360° about the axis. A structured mesh with 24237 cells, 48790 faces and 24554 nodes are used in the computational domain. To check whether the size of grid is sufficient, grid independence study has been done. As it is shown in Fig. 3 simulation with 24237 cells and 152334 cells, creates less than 0.1 % variation in the magnitude of concentration in the centreline of vitreous. This

N. Haghjou is with the Sharif University of Technology, Tehran, Iran (e-mail: haghjou@che.sharif.ir).

M. J. Abdekhodaie is with Sharif University of Technology, Tehran, Iran (e-mail: abdmj@sharif.edu).

Y. L. Cheng is with the Chemical Engineering and Applied Chemistry, University of Toronto, Toronto, Ontario, Canada, (e-mail: yuling.cheng@utoronto.ca).

good agreement between the solutions from the two grid levels justifies the use of 24237 cells for the simulation.

#### IV. GOVERNING EQUATIONS

Most previous studies assumed that the vitreous humor was stagnant, ignoring convective drug transport within the vitreous humor. Today, we know that mass transport in the vitreous humor is caused by both diffusion and convection. Convection arises because of steady permeating flow through the vitreous driven by a pressure drop between the anterior (hyaloid membrane) and the posterior (retina) surfaces and/or by active transport through the retina [7]. The moving fluid is considered to be the aqueous humor which is secreted from ciliary body and enters the vitreous cavity through the retrozonular and retrolental spaces as shown in Fig. 4[8]. Davson points out that the aqueous and vitreous humor is almost identical [9], giving support for the assumption that it is aqueous humor that moves through the vitreous body. The pressure source will be taken as the intraocular pressure; the pressure sink will be episcleral tissue on the outer surface of the eyeball. Part of the aqueous humor, at the intraocular pressure will be assumed to enter the vitreous body from the hyaloid membrane. Liquid leaves by flowing radially outward through the retina. In order to model the flow of fluid in the vitreous, it is assumed that no significant compression occurs under normal conditions in the vitreous, so the incompressible porous medium equations (Darcy law) were applied (1 & 2). According to Darcy's law, in laminar flows through porous media, the pressure drop is typically proportional to velocity as bellow:

Darcy's law:

$$\vec{v} = -\frac{K}{\mu} \nabla P \quad (1)$$

$$\nabla \cdot \vec{v} = 0 \rightarrow \nabla^2 P = 0 \quad (2)$$

where  $\vec{v}$  is the velocity of the fluid,  $K$  is the hydraulic conductivity of the vitreous,  $\mu$  is the viscosity of the fluid and  $P$  is the pressure. The flow is assumed to be steady and independent of the drug concentration.

To obtain the drug distribution, the standard convection-diffusion is solved:

$$\frac{\partial C}{\partial t} + \vec{v} \cdot \nabla C - D \nabla^2 C = 0 \quad (3)$$

where  $C$  is the concentration of the drug,  $D$  is the diffusion coefficient of drug in the vitreous. Species mass conservation equation (3), consists of both convection term ( $\vec{v} \cdot \nabla C$ ) and diffusion term ( $D \nabla^2 C$ ).

#### V. BOUNDARY CONDITIONS

There are three main tissues that bound the vitreous humor: the retina, lens, and hyaloid membrane. Boundary conditions are described here in detail and summarized in Table 1.

##### A. Hyaloid membrane

The hyaloid membrane (HM) separates the vitreous humor from the aqueous humor and the anterior segment of the eye. As considered by J. Xu (5) and Kathawate [10], the concentration is set to zero i.e.,  $C = 0$  at the hyaloid membrane. This boundary condition is based on the assumption that the aqueous flow rate is high relative to the release of the drug to the anterior segment. Pressure at the hyaloid membrane is considered to be the same as that of aqueous humor, which is close to the intraocular pressure (IOP) of the eye. During the pathogenesis of glaucoma, IOP is increased due to the obstruction of the pathway for the aqueous outflow. For a healthy human eye, IOP is generally between 15 and 20 mmHg (2000-2666 Pa), whereas for a glaucomatous eye it can rise up to 40-80 mmHg (5333-10666 Pa) [11]. In this study, pressure on hyaloid membrane is considered to be 2000 Pa for normal eye.

##### B. Lens

The lens is assumed to be impermeable to both flow and the drug concentration. Therefore, at the surface of the lens a no-flux boundary condition for concentration and no slip boundary condition for flow have been applied. However, the assumption of lens impermeability with respect to drug could be relaxed if one were interested in a drug capable of entering the lens [12].

##### C. Retina

Retina is covered by several layers as shown in Fig. 5, which give it mechanical support. Liquid leaving the vitreous chamber passes first through the retina, then the pigment epithelium, then through a loose capillary bed (the choroid and suprachoroid), then through the sclera, and finally through the loose episcleral tissue covering the eye.

The posterior eye layers are considered as a membrane. The boundary condition for momentum equation can be expressed by using Darcy's law as below:

$$n \cdot \vec{v} = n \cdot (-K_{RCS} \nabla P) = K_{RCS} \frac{(P - P_v)}{L}$$

where  $K_{RCS} = 15 \times 10^{-16} \text{ m}^2/\text{Pa}\cdot\text{s}$ , is total hydraulic conductivity of retina, choroid and sclera membrane (RCS),  $P_v$  is the pressure of the episcleral tissue (=1200 Pa) and  $L$  is RCS thickness which is considered to be 0.03 cm [13].

For the concentration boundary condition, we consider both convective and diffusive transport of the drug in general. The rate of diffusive flux on the boundary is (see Fig. 6):

$$J_D = -D_r \frac{\partial C}{\partial n} = D_r \frac{(C_{retina(0)} - C_{retina(1)})}{L} = D_r \frac{(kC_{retina} - kC_{choroid})}{L} = \frac{kD_r}{L} (C_{retina} - C_{choroid}) = P(C_{retina} - C_{choroid}) = PC_{retina}$$

where "k" is partition coefficient of the drug between vitreous and retina, "Dr" is diffusion coefficient of drug in the retina membrane; "L" is thickness of retina, " $C_{retina(0)}$ " is drug concentration on retina (vitreous side) and  $C_{retina(1)}$  is drug concentration in the other side of retina(choroid side). Choroid

layer is highly vascularized, so a reasonable assumption is that choroid will act as a perfect sink for drug transport across the retina, i.e.  $C_{\text{choroid}}=0$ . The value of  $kD_r/L$  is usually called retina permeability and is displayed by  $P$ .

The convective transport of drug, is expressed as below:

$$J_v = n \cdot \bar{v} C_{\text{retina}(0)} = n \cdot \bar{v} k C_{\text{retina}}$$

where  $n \cdot \bar{v}$  is the fluid velocity normal to the retina and  $k$  is the vitreous/retin partition coefficient. So, the concentration boundary condition on the retina is expressed as below:

$$n \left( -D \frac{\partial C}{\partial n} + \bar{v} C \right) = PC + n \cdot \bar{v} k C$$

## VI. INITIAL CONDITIONS

To model an intravitreal bolus injection of a specific value of drug, it is assumed that the drug is injected at the center of the vitreous chamber and that the injected drug initially has a homogenous distribution within a spherical region after injection. The initial size of the spherical region is assumed to be 1.3 mm in radius. The density of the drug is considered to be same as that of water i.e., 1000 kg/m<sup>3</sup>. The initial normalized mass fraction of the drug is assumed to be 1 (normalized with respect to the concentration of the drug in the water base) within the domain of the drug injection site while it is 0 in rest of the vitreous. In mathematical words:

$C_{t=0} = 1$  in the sphere of drug source

$C_{t=0} = 0$  outside of the drug source

## VII. COMPUTER CODE

The commercial code FLUENT 6.3 is used in this study. This code is based on a control volume approach where the computational domain is divided to a number of cells and the governing equations are discretized into algebraic equations in each cell. These equations satisfy the integral conservation of the mass and the momentum over each control volume.

## VIII. MODEL PARAMETERS

Intravitreal drug distribution depends on many parameters. Some of these parameters are related to the physicochemical specification of the drug, some are related to the eye physiology. The diffusivity of small molecules, such as gentamicin, fluorescein and fluorescein glucuronide in the vitreous humor has been found experimentally by Araie et al. [14] to be  $6 \times 10^{-10}$  m<sup>2</sup>/s, whereas for larger molecule drugs such as FITC-Dextran, the diffusivity is found to be  $3.9 \times 10^{-11}$  m<sup>2</sup>/s [15]. Retinal permeability (RP) varies depending on the physiological state of the retina and drug characteristics such as hydrophilicity or lipophilicity and molecular size that influence passive transport out of the eye. For example the retinal permeability of fluorescein has been measured to be  $2.6 \times 10^{-7}$  m/s and the retinal permeability of FITC-Dextran has been shown to be about  $1 \times 10^{-10}$  m/s. The parameters required to solve the model are summarized in Table 2.

## IX. RESULT AND DISCUSSION

### A. Velocity and Pressure Profiles

Most of previous studies assumed that the vitreous humor was stagnant, ignoring convective drug transport within the vitreous humor. However, the vitreous outflow can be an important factor that influences drug distribution within the eye especially for drugs with low vitreous diffusivity. Fig. 7 shows the speed contour in the normal eye. The average velocity at the retinal surface and in the vitreous chamber is  $7.8 \times 10^{-9}$  m/s and  $8.5 \times 10^{-9}$  m/s respectively. The total volumetric flow rate of aqueous humor through the vitreous body is 0.1  $\mu$ L/min, which is 4.5% of the total aqueous humor produced. Fig. 8 shows the pressure contour for a healthy eye. The pressure is, as specified, highest at the hyaloid membrane, and it decreases monotonically through the vitreous. The model predicts a steady permeating flow down the pressure gradient from the anterior to the posterior vitreous. The pressure drop across the vitreous is about 1 Pa, indicating that almost all of the pressure drop between the aqueous humor (2000 Pa) and the episcleral tissue (1200 Pa) occurs across the RCS.

### B. Drug Distribution and Elimination

Figs. 9-11 and Figs. 12-14 show the model-predicted concentration profiles for fluorescein and FITC-Dextran at 5hrs, 15hrs and 24hrs after a central injection respectively. For the fluorescein, the concentration contour lines are parallel to the retina as expected, because the fluorescein retinal permeability is high. Therefore, the retina is the dominant elimination mechanism. For the FITC-dextran, the model-predicted concentration contour lines are perpendicular to the retina, showing that drug is eliminated mainly via hyaloid membrane. The macula, which is located approximately in the center of the retina (see Fig. 1), is a highly sensitive part of the retina and is responsible for detailed central vision. Drug concentrations achievable at the macula are relevant for the treatment of retinal diseases, such as macular degeneration. Figs 15, 16 and 17 show time variation of drug concentration at 3 different sites: 1- macula, 2- adjacent to the lens and 3- mean vitreous concentration. The peak concentration observed in Fig. 15 shows that retina act as a limiting barrier to the drug transport and limits the rate of elimination. The drug diffuses to the retina, but can't be transferred across the retina with the same rate, leading to a high concentration adjacent to the retina. The peak concentration of FITC-Dextran is about 2 times more than that of fluorescein. This difference can be justified by comparison of retinal permeability (RP) to vitreous diffusivity ratio as below:

$$\text{Fluorescein} : \frac{RP}{D} = \frac{2.6 \times 10^{-7}}{6 \times 10^{-10}} = 433.3$$

$$\text{FITC - Dextran} : \frac{RP}{D} = \frac{1 \times 10^{-10}}{3.9 \times 10^{-11}} = 2.56$$

The above mentioned ratio is about 170 times greater for fluorescein with respect to that of FITC-Dextran. Therefore less peak concentration of fluorescein on macula compare to that of FITC-Dextran is justifiable. Also, it is seen in Fig. 15,

that the time required for the drug molecules to travel from the drug injection site to the retinal surface is much more for FITC-Dextran than that of fluorescein. The times to reach the maximum concentration on macula for fluorescein and FITC-Dextran are 1 hr and 19.5 hrs respectively. This difference can be attributed to lower vitreous diffusivity of FITC-Dextran compared to that of fluorescein.

Fig. 16 shows that maximum concentration in the vitreous adjacent to the lens is just slightly different between fluorescein and FITC-Dextran. However, the time at which the maximum concentration occurs, is much later for FITC-Dextran than fluorescein. This is consistent with our expectation, because the average time required for a drug to reach the lens increases as drug diffusivity decreases. Fig. 17 compares the mean vitreous concentration of fluorescein and FITC-Dextran. It is observed that fluorescein is rapidly cleared from the vitreous with a half-life of about 4.3hrs, whereas at this time only 2 % of FITC-Dextran is cleared. Therefore, drugs with physiochemical specification such as fluorescein need to be injected more frequently than drugs with properties similar to that of FITC-Dextran. Multiple injections are not only inconvenient for patients, but also increase the risk of ocular complications such as vitreous hemorrhage, retinal detachment, endophthalmitis and cataract (16). These drugs are good candidates for sustained-release drug delivery systems. The values of above mentioned pharmacokinetic parameters such as drugs' vitreous half-life and mean vitreous concentration as well as maximum concentration on different tissues surrounding the vitreous are summarized in Table 3. All concentrations mentioned in Table 3 have been normalized with respect to the injected drug concentration. The initial drug concentration in the vitreous (just after injection) is 0.0066 for both drugs.

### C. Experimental Validation

Araie and Maurice (14) reported the normalized concentration of fluorescein between lens and retina of rabbit eye along the symmetrical axis 15hrs after intravitreal injection. Fig. 18 shows the comparison of the present numerical results with their experimental data. Fluorescein concentration has been normalized with respect to the concentration found next to the lens. The difference between the numerical calculation and the experimental result of Araie and Maurice is less than 5%. This validation provides strong support for the numerical methodology and associated assumptions of the current study.

### X. CONCLUSION

A finite volume model of intravitreally administered drugs has been developed to predict drug distribution in the vitreous. The accuracy of simulation depends largely on the eye geometry, the vitreous and surrounding tissues properties and the boundary conditions used in the simulation. The good compliance of model-predicted concentrations with available experimental data provides strong support for correctness of the developed model. The mathematical model can be used to predict drug effectiveness and toxicity on different intraocular tissues. In addition to that, simulation allows the user to more

quickly test and optimize the design of products, whilst offering greater insight and understanding. Modeling helps choosing the best form of drug administration and the most effective utilization of each injection. Therefore frequency of injection and complications can be minimized. Although modeling does not entirely eliminate the necessity for experimental work, it does provide quick and cost effective evaluations of new drug formulations and the performance sensitivity of drug delivery system to changes in parameters.

### REFERENCES

- [1] J. E. Chastain, "General considerations in ocular drug delivery," in: *Ophthalmic Drug Delivery Systems*, A. K. Mitra, Ed. New York: Marcel Dekker, 2003, p. 76.
- [2] E. Eljarrat-Binstock E, J. Pe'er and A. J. Domb, "New techniques for drug delivery to the posterior eye segment," *Pharm Res.*, vol. 27 (4). 2010, pp. 530-543.
- [3] G. A. Peyma, M. E. Lad and M. D. Moshfeghi, "Intravitreal injection of therapeutic agents," *Retina, The journal of retina and vitreous diseases*, vol. 29(7) 2009, pp. 875-911.
- [4] C. Duraira, J. C. Sha, S. Senapati and U. B. Kompella, "Prediction of vitreal half-life based on drug physicochemical properties: quantitative structure-pharmacokinetic relationships (QSPKR)," *Pharm. Res.*, vol. 26(5) 2009, pp. 1236-1260.
- [5] M. S. Sta, J. X, T. W. Randolph and V. H. Barocas, "Computer simulation of convective and diffusive transport of controlled release drugs in the vitreous humor," *Pharm. Res.*, vol. 20,2003, pp. 96-102.
- [6] S. Friedrich, Y. L. Cheng and B. Saville, "Finite element modelling of drug distribution in the vitreous humor of the rabbit eye," *Ann. Biomed. Eng.* vol. 25,1997, pp. 303-314.
- [7] J. Xu, J. J. Heys, V. H. Barocas and T. W. Randolph, "Permeability and diffusion in vitreous humor: implications for drug delivery," *Pharm. Res.*, vol. 17, 2000, pp. 664-669.
- [8] E. N. Marieb and K. Hoehn, *Human Anatomy & Physiology*, 7th ed., Pearson Education Inc, 2006.
- [9] H. Davson, in: *The Eye*, 2<sup>nd</sup> ed., H. Davson, Ed., New York: Academic Press, 1969, pp. 88-92
- [10] J. Kathawate and S. Acharya, "Computational modeling of intravitreal drug delivery in the vitreous chamber with different vitreous substitutes," *International Journal of Heat and Mass Transfer*, vol. 5, 2008, pp. 5598-5609.
- [11] P. L. Kaufman and A. Alm, *Adlers's Physiology of the Eye*, 10th ed. Mosby Year book, 2003.
- [12] P. A. Pearson, G. J. Jaffe, D. F. Martin, G. J. Cordahi, H. Grossniklaus, E. T. Schmeisser and P. Ashton, "Evaluation of a delivery system providing long-term release of cyclosporine," *Arch. Ophthalmol.* vol. 114, 1996, pp. 311-317.
- [13] I. Fatt and B. Hedbys, "Flow of water in the sclera," *Exp. Eye Res.* Vol. 10, 1970, pp. 243-249.
- [14] M. Araie and D. M. Maurice, "The loss of fluorescein, fluorescein glucuronide and fluorescein isothiocyanate dextran from the vitreous by the anterior and retinal pathways," *Exp. Eye Res.*, vol. 52, 1991, pp. 27-39.
- [15] L. Pitkänen, V. Ranta, V. H. Moilanen and A. Urtti, "Permeability of Retinal pigment epithelium: effects of permeant molecular weight and lipophilicity," *Invest. Ophthalmol. Vis. Sci.* vol. 46,2005, pp. 641-646.
- [16] D. Maurice, "Review: practical issues in intravitreal drug delivery," *J Ocul Pharmacol Ther.* Vol. 17(4), 2001, pp. 393-401.

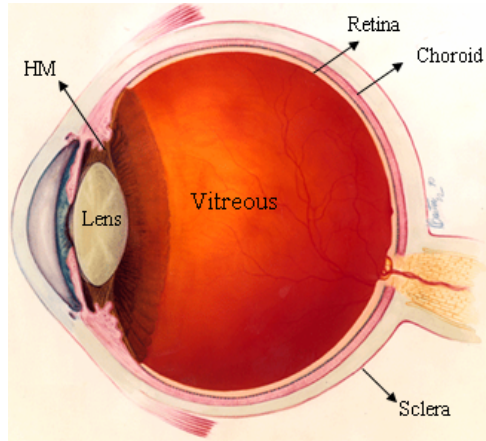


Fig. 1 Anatomy of the human eye

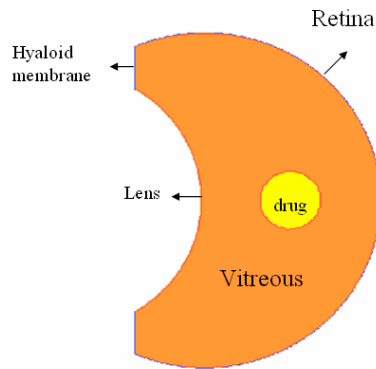


Fig. 2 Geometrical model based on rabbit eye dimension

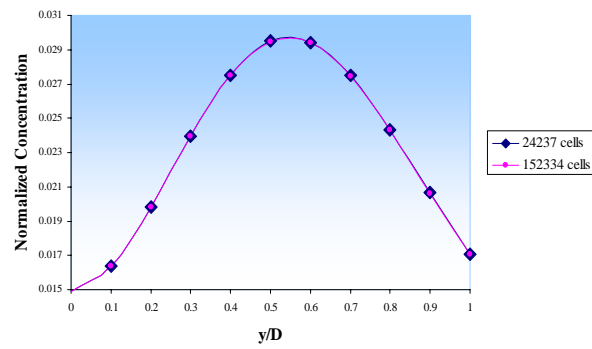


Fig. 3 Normalized concentration along the center of vitreous chamber for 24,237 & 152,334 cells

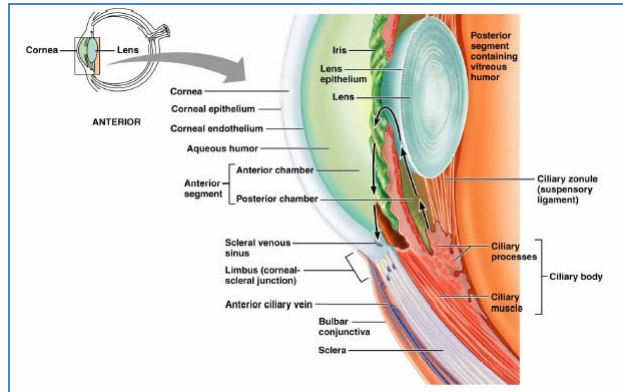


Fig. 4 Secretion of ocular humors from ciliary body

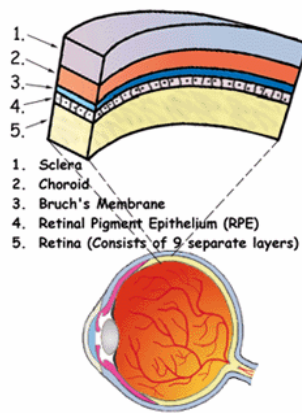


Fig. 5 Schematic view of posterior eye layers

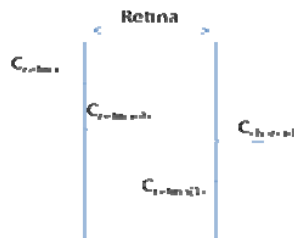


Fig. 6 Schematic of drug concentration on retina layer

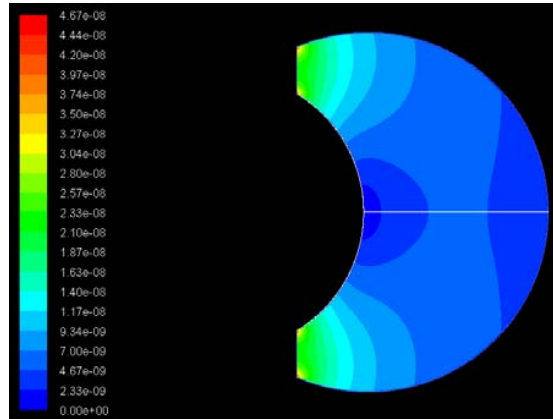


Fig.7 Speed contour in the posterior segments of the rabbit eye model (IOP=2000 Pa)

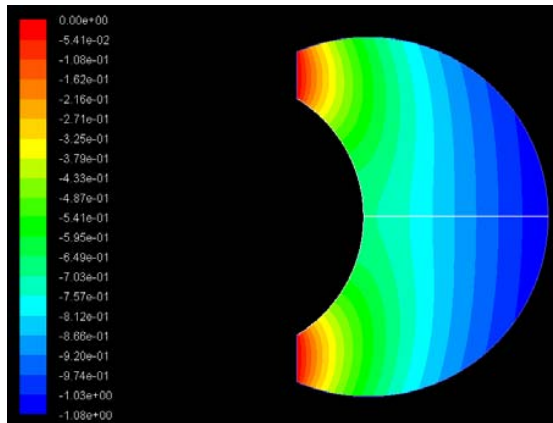


Fig.8 Pressure contour in the vitreous

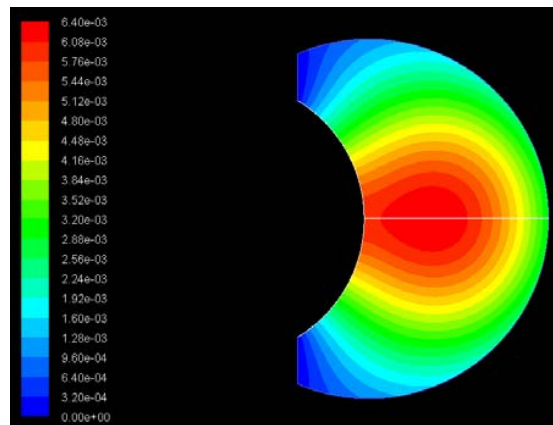


Fig.9 Concentration contour 5hrs after injection of Fluorescein

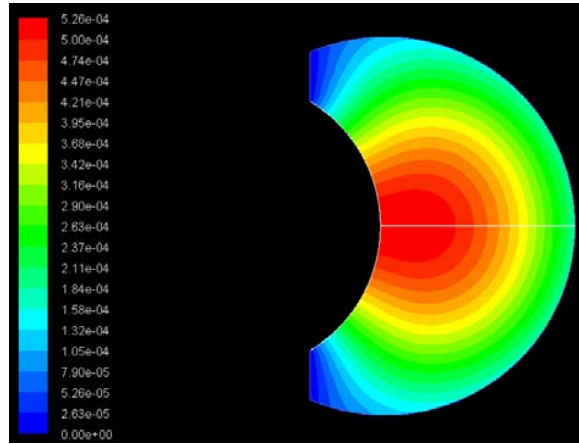


Fig.10 Concentration contour 15hrs after injection of Fluorescein

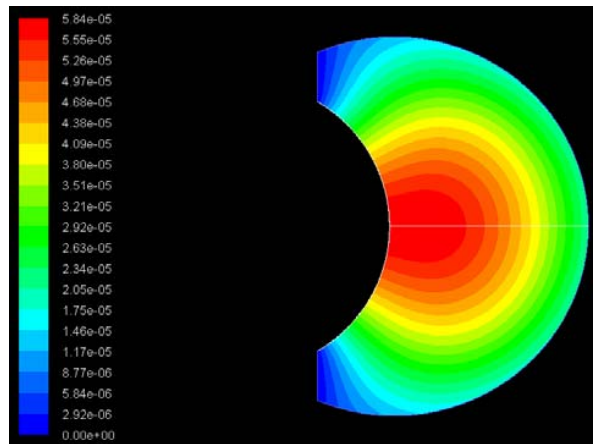


Fig.11 Concentration contour 24hrs after injection of Fluorescein

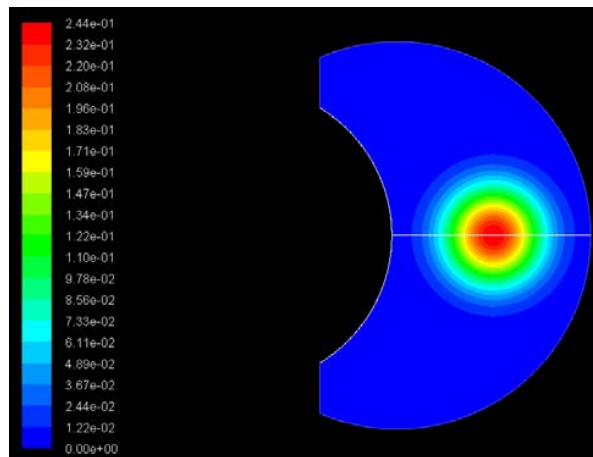


Fig.12 Concentration contour 5hrs after injection of FITC-Dextran



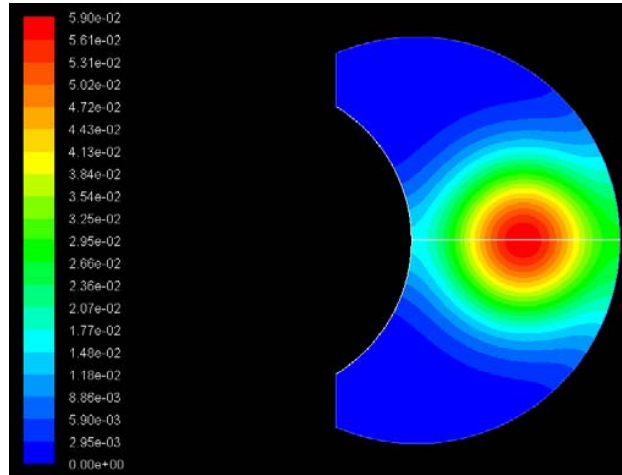


Fig.13 Concentration contour 15hrs after injection of FITC-Dextran

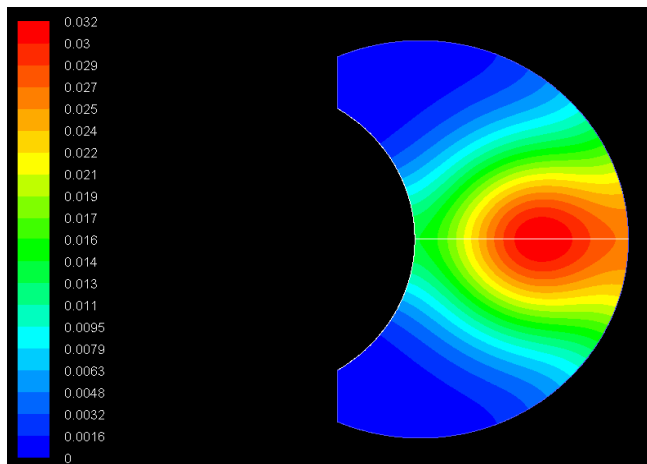


Fig.14 Concentration contour 24hrs after injection of FITC-Dextran

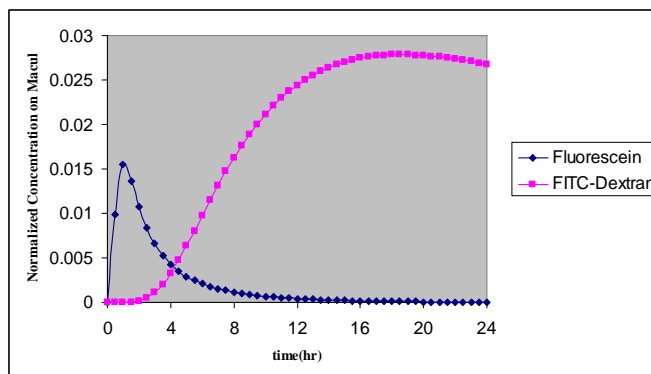


Fig.15 Drug concentration at Macula

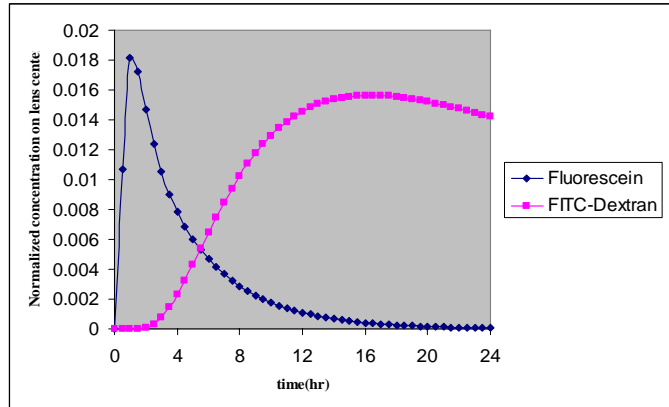


Fig.16 Drug concentration adjacent to the Lens

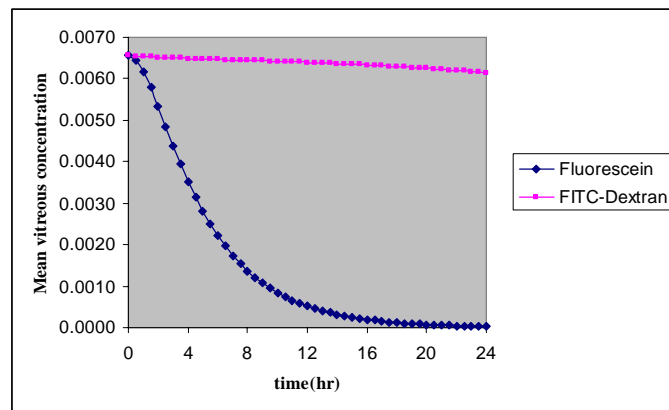


Fig.17 Mean vitreous drug concentration

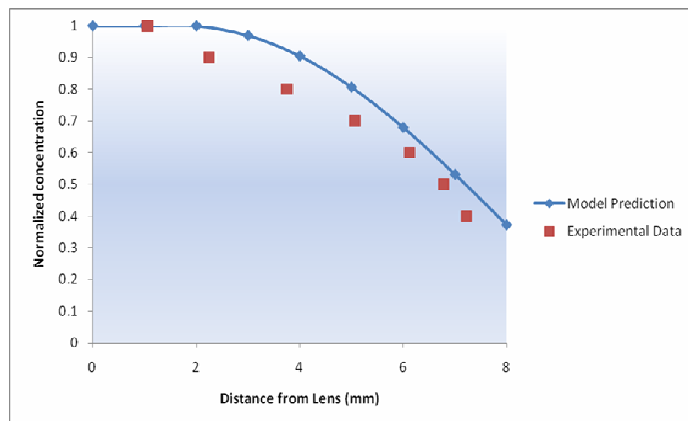


Fig.18 Comparison of numerical result and experimental data at 15 hrs after intravitreal injection

TABLE I  
SUMMARY OF BOUNDARY CONDITIONS

Boundary name	Momentum Eq.	Mass Transfer Eq.
Hyaloid membrane	$P = 2000Pa$	$C = 0$
Retina	$n \cdot \vec{v} = K_{RCS} \frac{(P - P_v)}{L}$	$n \left( -D \frac{\partial C}{\partial n} + \vec{v} C \right) = PC + n \cdot \vec{v} k C$
Lens	$\vec{v} = 0$	$\frac{\partial C}{\partial n} = 0$
Axis	$n \cdot \vec{v} = 0$	$\frac{\partial C}{\partial n} = 0$

TABLE II  
MODEL PARAMETERS

PARAMETER	UNIT	VALUE
Viscosity of vitreous humor [16]	$kg\ m^{-1}\ s^{-1}$	$6.9 \times 10^{-4}$
Hydraulic conductivity in the vitreous [8]	$m^2\ pa^{-1}\ s^{-1}$	$8.4 \times 10^{-11}$
Hydraulic conductivity of RCS [15]	$m^3\ Pa^{-1}\ s^{-1}$	$1.5 \times 10^{-15}$
Partition coefficient (vitreous/retina) [4]	----	7.9 (Fluorescein) 0.4 (FITC-Dextran)
Vitreous Diffusivity [16,17]	$m^2/s$	$6 \times 10^{-10}$ (Fluorescein) $3.9 \times 10^{-11}$ (FITC-Dextran)
Retinal Permeability [16]	$m/s$	$2.6 \times 10^{-7}$ (Fluorescein) $1 \times 10^{-10}$ (FITC-Dextran)
IOP	Pa	2000

TABLE III  
MODEL-PREDICTED PHARMACOKINETIC PARAMETERS FOR FLUORESCIN AND FITC-DEXTRAN

DRUG	VITREOUS HALF-LIFE	MEAN VITREOUS CONCENTRATION		PEAK CONCENTRATION	
		5hrs	15hrs	Macula	Lens Center
Fluorescein	4.2 hrs	0.0028	0.00025	0.015	0.018
FITC-Dextran	11days	0.0065	0.0063	0.029	0.016